

## Chemical Enhancement by Nanomaterials under X-ray Irradiation

Neal N. Cheng, Zane Starkewolf, R. Andrew Davidson, Arjun Sharmah, Changju Lee, Jennifer Lien, and Ting Guo\*

Department of Chemistry, University of California, Davis, California 95616, United States

**S** Supporting Information

**ABSTRACT:** We report here a new phenomenon of dynamic enhancement of chemical reactions by nanomaterials under hard X-ray irradiation. The nanomaterials were gold and platinum nanoparticles, and the chemical reaction employed was the hydroxylation of coumarin carboxylic acid. The reaction yield was enhanced 2000 times over that predicted on the basis of the absorption of X-rays only by the nanoparticles, and the enhancement was found for the first time to depend on the X-ray dose rate. The maximum turnover frequency was measured at  $1 \times 10^{-4} \text{ s}^{-1} \text{ Gy}^{-1}$ . We call this process chemical enhancement, which is defined as the increased yield of a chemical reaction due to the chemical properties of the added materials. The chemical enhancement described here is believed to be ubiquitous and may significantly alter the outcome of chemical reactions under X-ray irradiation with the assistance of nanomaterials.

X-ray absorption by materials has been broadly used in imaging, lithography, and treatment since the discovery of X-rays. Nanomaterials, which were widely used as catalysts decades ago, are being intensely explored in many fields, especially biology. The use of previously considered inert nanomaterials such as gold nanoparticles to increase the absorption of X-rays began a few years ago, and many chemical and biological responses have been used to quantify the enhancement.<sup>1,2</sup> Because gold nanoparticles can be catalytically active under suitable conditions,<sup>3–9</sup> it is likely that these nanomaterials may do more than simply enhance the absorption of X-rays in a highly reactive environment such as those created by X-ray radiation. However, all of the observed enhancements to date have been attributed to physical properties of the nanomaterials, i.e., high atomic numbers, leading to increased X-ray absorption and subsequent increased generation of reactive oxygen species (ROS), even though the observed enhancements could be much higher than the values predicted on the basis of the physical enhancement at low loadings (<0.1 wt %) of nanoparticles<sup>1,10</sup> or much lower at high loadings (~1 wt %) of nanoparticles.<sup>11</sup> These disagreements indicate that physical enhancement alone, even taking into account reabsorption of emitted secondary photons and electrons,<sup>12</sup> which is negligible, cannot explain the observed enhancement. Here we introduce a new concept, chemical enhancement, that is enabled by both the radiation-generated ROS and the surface of the nanomaterials. The concept discovered here may also be useful in applications such as energy production, nuclear waste processing, radiation

chemistry, chemical synthesis, radiotherapy, catalysis, sensing, nanotoxicity, and nanomedicine.

Figure 1 shows several nanomaterials synthesized and employed here, including  $2.0 \pm 0.4 \text{ nm}$  platinum nanoparticles

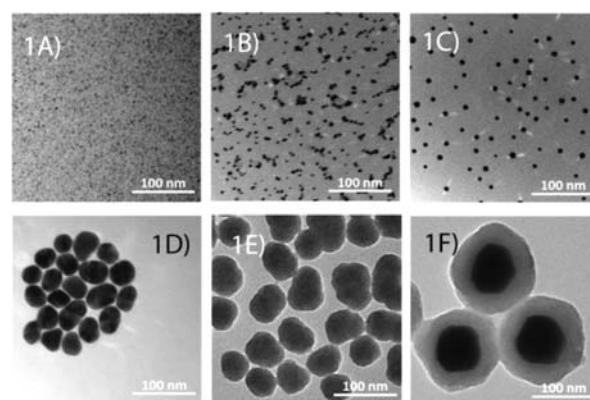


**Figure 1.** TEM images of (A) 1.7 nm PtNPs; (B–D) 3, 7, and 30 nm AuNPs; (E) silica NPs (40 nm); and (F) silica-coated AuNPs (72 nm Au core, 29 nm thick silica shell).

(PtNPs),  $3.8 \pm 1.0 \text{ nm}$  (denoted as “3 nm” in the text),  $7.0 \pm 1.3 \text{ nm}$  (“7 nm”), and  $35.2 \pm 4.9 \text{ nm}$  (“30 nm”) gold nanoparticles (AuNPs),  $53 \pm 6.4 \text{ nm}$  silica nanoparticles, and nanoparticles having a  $72.6 \pm 4.6 \text{ nm}$  gold core and a  $28.8 \pm 4.0 \text{ nm}$  thick silica shell. Figure 2A shows the increased production of highly fluorescent 7-hydroxycoumarin-3-carboxylic acid (7-OH-CCA) from hydroxylation of weakly fluorescent coumarin-3-carboxylic acid (3-CCA) as a function of AuNP concentration for the three nanoparticle sizes shown in Figure 1B–D (3, 7, and 30 nm). The increase is expressed as the enhancement of the yield of 7-OH-CCA caused by AuNPs, which is defined as the ratio of the fluorescence signal of 7-OH-CCA with AuNPs to that without AuNPs minus 1. Thus, an enhancement value of 0 means no increase to the yield, and an enhancement value of 1.0 means a 100% increase. The lowest concentration to observe a 10% enhancement was less than 0.5 ppm or 20 nM for the 3 nm AuNPs, 3 ppm or 2.4 nM for 7 nm AuNPs, and 25 ppm or 0.15 nM for 30 nm AuNPs. Because the reaction is used as a dosimetry reaction, naturally such an enhancement would be interpreted as an increase in OH-production, which would be incorrect because AuNPs actually played an active and chemical role. As the amount of AuNPs in

Received: October 31, 2011

Published: January 19, 2012

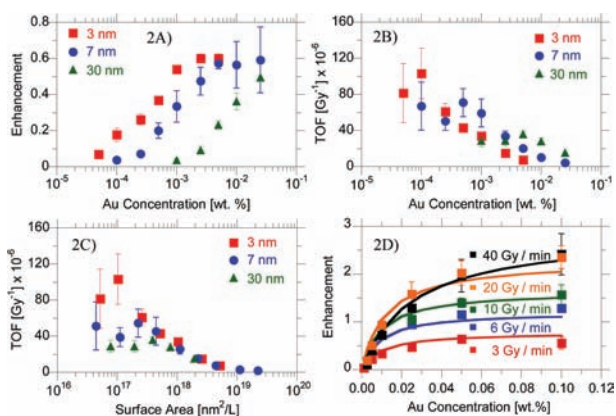


**Figure 2.** Chemical enhancement results. (A) Enhancement as a function of AuNP concentration for the three sizes of AuNPs. Enhancement was observed below 1 ppm. (B) TOF for these three sizes of AuNPs. (C) TOF as a function of the total surface area. (D) Dose rate dependence of the absolute enhancement for 7 nm AuNPs. The experimental data are shown as symbols and the theoretical simulations (see the text) as solid lines. The dose rate dependence reached saturation above 20 Gy/min. The simulations were based on a model proposing that the activity of the AuNPs comes from superoxide produced by X-ray radiation.

solution increased to >0.1 wt %, which is the value needed to generate ~10% physical enhancement (PE) (see below), the experimentally measured enhancements started to decrease and even became negative (i.e., antienhancement; data not shown), which implies that these nanoparticles or their surfactants begin to scavenge OH· at high enough AuNP or PtNP concentrations.<sup>13</sup> This scavenging process may be the cause of the observed low enhancement at high loadings of nanoparticles. However, scavenging is negligible at sufficiently low concentrations (<0.1 wt %) of AuNPs, as shown in Figure 2. The enhancements reached a maximum of 0.6 (60%) at an X-ray irradiation dose rate of 3.3 Gy/min. If this is a catalytic reaction, then on the basis of Figure 2A, the traditionally defined parameter of turnover frequency (TOF), which is the number of chemical reactions catalyzed by a surface atom in nanoparticles per second, can be calculated. Figure 2B shows that the TOF reached the highest values at the lowest concentrations for each of the three sizes of nanoparticles and then gradually decreased as the concentration of nanoparticles increased. Such a decrease in TOF with increasing total surface area suggests that there is a limiting reagent other than the surface area of AuNPs. On the basis of the data shown in Figure 2A,B over a large range of concentrations, it appears that there is a size dependence. The prominence of this feature subsided when the TOF data were plotted as a function of the total surface area (Figure 2C), although the 3 nm AuNPs still seemed to be better than the 30 nm AuNPs by a factor of 2 at the lowest surface areas. The TOF reached a plateau at the maximum value of nearly  $1 \times 10^{-4} \text{ s}^{-1} \text{ Gy}^{-1}$  at a dose rate of 3.3 Gy/min for 3 nm AuNPs with minimum total surface areas. This weak size independence, which exists for several catalytic systems,<sup>14</sup> is characteristically different from the catalytic properties of small AuNPs, indicating that the mechanism of enhancement is different from that causing the oxidation of CO by small AuNPs on substrates.<sup>3</sup>

To test whether the observed activity truly originated from the surface of gold and not from poly(ethylene glycol) (PEG)

or other ligands covering the AuNPs or even just any type of nanoparticle, we synthesized and employed pure silica nanoparticles and silica-shell-covered AuNPs (Figure 1E,F). There was almost no scavenging or enhancement at already high nanoparticle concentrations. PEG-covered silica nanoparticles were also tested, and no enhancement was observed, proving that enhancement does not happen for nanoparticles in general [see Figure SI-1 in the Supporting Information (SI)]. This result also reconfirmed that previously claimed re-emission or absorption of secondary X-rays did not cause the enhancement.<sup>12</sup> On the other hand, for an equal amount of AuNPs, there was measurable enhancement, as shown in Figure 2A. This proves that the enhancement observed in Figure 2A–C was due to the surface gold atoms of the AuNPs and not to the bulk gold atoms or surface atoms of nanoparticles in general. We also synthesized and employed several other nanoparticles, including Ag, Pt, CdTe, and TiO<sub>2</sub> nanoparticles. PtNPs (2 nm) covered with poly(vinylpyrrolidone) (PVP) ligands showed similar enhancement as AuNPs. On the other hand, no enhancement was observed over a large span of concentrations for 15 nm AgNPs, suggesting that a plasmonic phenomenon is not the cause of the enhancement.<sup>4</sup> CdTe nanoparticles (3 nm) were also synthesized and used, and no enhancement was detected at a dose rate of 3.3 Gy/min. Large-band-gap semiconductor TiO<sub>2</sub> nanoparticles alone under X-ray irradiation did not cause enhancement either.

We employed excessive amounts of sodium azide, sodium nitrate, superoxide dismutase (SOD), and ascorbic acid to determine the chemical species responsible for the enhancement. Sodium azide was used to scavenge singlet oxygen preferentially, and the enhancement was unchanged with the addition of up to 1 mM sodium azide, proving that singlet oxygen was not responsible for the enhancement. On the other hand, 0.5 mg/mL SOD or 0.5 mM ascorbic acid quenched the enhancement. Ascorbic acid scavenges OH, superoxide, and singlet oxygen, whereas SOD removes only superoxides effectively. These results suggest that the enhancement relies on superoxides. Sodium nitrate aqueous solution was employed to test the role of solvated electrons, and no detectable changes were found.

On the basis of these investigations, we hypothesize that weakly electronegative metal surfaces free of oxides, such as those of AuNPs or PtNPs, may be necessary for the enhancement observed here.<sup>4</sup> Superoxides are also required; their role may be to transfer electrons to the AuNPs or PtNPs to make them anionic, allowing OH radical-adduct intermediates 3-OH-CCA· to react on the surface to form 7-OH-CCA either sequentially or simultaneously. If these hypotheses are true, then the enhancement should increase as a result of simultaneously increasing the concentration of intermediates and the total surface area of the nanomaterials. This could be done with more intense X-ray sources and greater nanoparticle concentrations. Figure 2D shows the results of enhancement measurements using a more intense microfocus X-ray source. The dose rate measurements showed that the enhancement was much improved at higher dose rates and high AuNP concentrations, eventually reaching 200% or 2-fold enhancement at 20 Gy/min with 0.1 wt % 7 nm AuNPs (square symbols for experimental data). The solid lines are theoretically predicted responses (see below). These results show that enhancement is dose-rate-dependent at high AuNP concentrations and suggest that the enhancement processes must

involve species such as superoxides that are generated by X-ray radiation.

The observed experimental data can be explained by reactions of radical intermediates 3-OH-CCA· with superoxide-activated AuNPs or PtNPs. Figure 3 shows the new

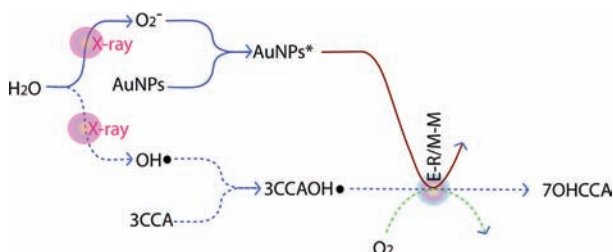


**Figure 3.** Proposed mechanisms for chemical enhancement. The proposed mechanism is a combination of the Michaelis–Menten (M–M) and Eley–Rideal (E–R) mechanisms. Two possible reaction pathways are shown: pathway 1 (dashed lines) is the previously established mechanism of formation of 7-OH-CCA, and pathway 2 (solid lines) displays the proposed superoxide-activated AuNP pathways. Pathway 2 employs OH· produced from AuNPs, but OH· from water would also be possible. O<sub>2</sub>, superoxide (O<sub>2</sub><sup>·-</sup>), OH·, 3-CCA, 3-OH-CCA· (radical), 7-OH-CCA (the product), and AuNPs are shown.

reaction pathway involving activation of the surface atoms in AuNPs by X-ray radiation-generated superoxides (solid lines). The originally proposed pathway in the literature is also shown (dashed lines).<sup>15</sup> The new pathway can be considered as a combination of at least two well-known catalytic reaction mechanisms. The radical intermediate 3-OH-CCA· can be regarded as the substrate in the traditional enzyme kinetics described in the Michaelis–Menten (M–M) framework, where AuNP–superoxide (AuNP–O<sub>2</sub><sup>·-</sup>) would be the designated enzyme. However, it is possible that an AuNP could become negatively charged upon reaction with a superoxide, and the negatively charged AuNP would enhance the reaction between 3-OH-CCA· and one of the O<sub>2</sub> molecules around the negatively charged AuNP (shown in Figure 3) to form 7-OH-CCA. This deviates from the original M–M picture but resembles a process described as the Eley–Rideal (E–R) mechanism because the reacting oxygen molecule comes to the surface of the AuNP to initiate the reaction. This combination hence represents a new mechanism that makes the enhancement dose-rate-dependent. Although 3-OH-CCA· may react with O<sub>2</sub> in water and the complex may migrate to the surface of AuNPs, this is unlikely because the lifetime of 3-OH-CCA–O<sub>2</sub> is fairly short.<sup>16</sup> The proposed mechanism is different from another previously proposed mechanism that suggests oxygen may interact with the gold surface to form superoxides;<sup>17</sup> if AuNPs could form superoxides without radiation as found in previous studies,<sup>17</sup> then the enhancement would be dose-rate-independent. We theoretically modeled the enhancement by establishing the rate equations for AuNPs, DMSO, O<sub>2</sub>, O<sub>2</sub><sup>·-</sup> and the dose rate (see eqs 1–6 in the SI). The AuNP concentration dependence shown in Figure 2A was reproduced, closely resembling that obtained based on the Langmuir–Hinshelwood formula with the modification that O<sub>2</sub> can be any of those around the AuNPs and not necessarily the adsorbed superoxide itself.<sup>18</sup> The solid lines in Figure 2D show the theoretically modeled results of the dose rate calculation, which agree with the experimental data. In addition, the concentration depend-

ence and nanoparticle size effect were also duplicated using this model (see Figures SI-3 and SI-4).

The chemical enhancement (CE) of the effect of X-ray radiation described here requires the activation of nanomaterials by superoxides produced under X-ray irradiation. Therefore, we call it dynamic CE. CE is different from physical enhancement (PE), which is defined as the increased absorption of radiation that leads to increased generation of ROS such as superoxides, OH·, and singlet oxygen as a result of the introduced materials under irradiation. PE hence enhances the X-ray absorption and therefore the energy deposition.<sup>19</sup> Many examples exist. For instance, AuNPs were employed to increase the cleavage of DNA strands through increased absorption of X-rays.<sup>2</sup> Nanoporous gold has been shown to enhance radiolysis of water.<sup>20</sup> Several recent experiments employed AuNPs for their PE property and observed enhanced damage to biological samples.<sup>21–23</sup> Theoretical works have also been carried out to explain the results in terms of the enhanced energy deposition from the added nanomaterials.<sup>19,24–26</sup> PE can be further divided into two categories. Average or remote PE, which we call type-1 PE, creates uniform enhancement in solution. A general rule of thumb is that adding 1 wt % gold (relative to water in the sample) creates ~140% increase in energy deposition. The observed CE for 3 nm AuNPs at 4 × 10<sup>-5</sup> wt % (Figure 2A) is hence 2000 times the predicted type-1 PE (Figure SI-5). Type-2 PE, a nanoscale or local physical enhancement, can be effective only when two conditions are simultaneously met: (1) the probe molecules (e.g., DNA) must be placed within nanometers of the nanomaterial (e.g., AuNPs) and (2) scavengers must be present to reduce the contribution of OH· from surrounding water.<sup>19</sup> However, neither condition was met here. Both types of PE can depend on the X-ray energy.<sup>27</sup> Another possibility is that superoxides may be converted to OH· and hydroperoxyl radicals by AuNPs (see the SI). However, the amount of OH· produced this way is considerably less than that produced from radiation of water, and only a very small amount of hydroperoxyl radicals exist at pH 7.0.<sup>28</sup> Furthermore, this mechanism could not reproduce the observed dose rate dependence shown in Figure 2D. As a result, both types of PE could not explain the enhancements measured here, and there is a negligible increase in ROS due to the introduction of nanoparticles. We hence conclude that the observed enhancement is solely caused by the increased conversion of intermediates to the products occurring on the surface of AuNPs or PtNPs.

The presented results show that only a small amount of AuNPs can cause significant changes in the outcome of radiation experiments. The proposed radiation-activated dynamic CE can also explain the previously observed enhancement in several studies in which a ~50% increase in the damage to biological samples was observed when <0.01 to 0.1 wt % AuNPs (uptake) was employed.<sup>11,29,30</sup> The observed enhanced damage could not be explained by PE, which at best could account for only a small fraction of the damage. On the other hand, on the basis of the work presented here, CE should be on the order of 50% at those AuNP concentrations, and the CE discovered here remains high in the presence of radical scavengers such as those abundant in cells. It is also possible that CE may lead to more complicated biological enhancement (BE), so the concept of CE may play an important role in understanding reactive environments such as cells where radiation-generated and naturally existing intermediates and

ROS-activated nanomaterials are abundant. Both CE and BE could be crucial for understanding nanotoxicity under radiation.

## ■ ASSOCIATED CONTENT

### ■ Supporting Information

Synthesis details, experimental protocols, theoretical methodology for modeling the CE, and additional experimental and theoretical results. This material is available free of charge via the Internet at <http://pubs.acs.org>.

## ■ AUTHOR INFORMATION

### Corresponding Author

[tguo@ucdavis.edu](mailto:tguo@ucdavis.edu)

## ■ ACKNOWLEDGMENTS

We thank Ms. Larissa Miyachi for her experimental assistance. This work was supported by the National Science Foundation (CHE-0957413).

## ■ REFERENCES

- (1) Hainfeld, J.; Slatkin, D.; Smilowitz, H. *Phys. Med. Biol.* **2004**, *49*, N309.
- (2) Foley, E.; Carter, J.; Shan, F.; Guo, T. *Chem. Commun.* **2005**, 3192.
- (3) Haruta, M.; Kobayashi, T.; Sano, H.; Yamada, N. *Chem. Lett.* **1987**, 405.
- (4) Garcia, H.; Navalon, S.; de Miguel, M.; Martin, R.; Alvaro, M. J. *Am. Chem. Soc.* **2011**, *133*, 2218.
- (5) Mirkin, C. A.; Zhang, K.; Cutler, J. I.; Zhang, J. A.; Zheng, D.; Auyeung, E. J. *Am. Chem. Soc.* **2010**, *132*, 15151.
- (6) Tsukuda, T.; Tsunoyama, H.; Ichikuni, N.; Sakurai, H. *J. Am. Chem. Soc.* **2009**, *131*, 7086.
- (7) Cao, R.; Cao, R.; Villalonga, R.; Diaz-Garcia, A. M.; Rojo, T.; Rodriguez-Arguelles, M. C. *Inorg. Chem.* **2011**, *50*, 4705.
- (8) Lambert, R. M.; Turner, M.; Golovko, V. B.; Vaughan, O. P. H.; Abdulkin, P.; Berenguer-Murcia, A.; Tikhov, M. S.; Johnson, B. F. G. *Nature* **2008**, *454*, 981.
- (9) Hutchings, G. J.; Hughes, M. D.; Xu, Y. J.; Jenkins, P.; McMorn, P.; Landon, P.; Enache, D. I.; Carley, A. F.; Attard, G. A.; King, F.; Stitt, E. H.; Johnston, P.; Griffin, K.; Kiely, C. J. *Nature* **2005**, *437*, 1132.
- (10) McMahan, S. J.; Hyland, W. B.; Muir, M. F.; Coulter, J. A.; Jain, S.; Butterworth, K. T.; Schettino, G.; Dickson, G. R.; Hounsell, A. R.; O'Sullivan, J. M.; Prise, K. M.; Hirst, D. G.; Currell, F. J. *Sci. Rep.* **2011**, *1*, 18.
- (11) Chithrani, D. B.; Jelveh, S.; Jalali, F.; van Prooijen, M.; Allen, C.; Bristow, R. G.; Hill, R. P.; Jaffray, D. A. *Radiat. Res.* **2010**, *173*, 719.
- (12) Misawa, M.; Takahashi, J. *Nanomedicine* **2011**, *7*, 604.
- (13) Shirahata, S.; Hamasaki, T.; Kashiwagi, T.; Imada, T.; Nakamichi, N.; Aramaki, S.; Toh, K.; Morisawa, S.; Shimakoshi, H.; Hisaeda, Y. *Langmuir* **2008**, *24*, 7354.
- (14) Qu, Y. Q.; Sutherland, A. M.; Lien, J.; Suarez, G. D.; Guo, T. J. *Phys. Chem. Lett.* **2010**, *1*, 254.
- (15) Lout, G.; Foley, S.; Cabillic, J.; Coffigny, H.; Taran, F.; Valleix, A.; Renault, J. P.; Pin, S. *Radiat. Phys. Chem.* **2005**, *72*, 119.
- (16) Bohn, B. J. *Phys. Chem. A* **2001**, *105*, 6092.
- (17) Ionita, P.; Gilbert, B. C.; Chechik, V. *Angew. Chem., Int. Ed.* **2005**, *44*, 3720.
- (18) Zhang, Z. Y.; Berg, A.; Levanon, H.; Fessenden, R. W.; Meisel, D. J. *Am. Chem. Soc.* **2003**, *125*, 7959.
- (19) Carter, J. D.; Cheng, N. N.; Qu, Y. Q.; Suarez, G. D.; Guo, T. J. *Phys. Chem. B* **2007**, *111*, 11622.
- (20) Renault, J. P.; Musat, R.; Moreau, S.; Poidevin, F.; Mathon, M. H.; Pommeret, S. *Phys. Chem. Chem. Phys.* **2010**, *12*, 12868.
- (21) Butterworth, K. T.; Coulter, J. A.; Jain, S.; Forker, J.; McMahan, S. J.; Schettino, G.; Prise, K. M.; Currell, F. J.; Hirst, D. G. *Nanotechnology* **2010**, *21*, 29.
- (22) Sicard-Roselli, C.; Brun, E.; Duchambon, P.; Blouquit, Y.; Keller, G.; Sanche, L. *Radiat. Phys. Chem.* **2009**, *78*, 177.
- (23) Hwu, Y.; Liu, C. J.; Wang, C. H.; Chen, S. T.; Chen, H. H.; Leng, W. H.; Chien, C. C.; Wang, C. L.; Kempson, I. M.; Lai, T. C.; Hsiao, M.; Yang, C. S.; Chen, Y. J.; Margaritondo, G. *Phys. Med. Biol.* **2010**, *55*, 931.
- (24) Pradhan, A. K.; Nahar, S. N.; Montenegro, M.; Yu, Y.; Zhang, H. L.; Sur, C.; Mrozik, M.; Pitzer, R. M. J. *Phys. Chem. A* **2009**, *113*, 12356.
- (25) Cho, S. H.; Jones, B. L.; Krishnan, S. *Phys. Med. Biol.* **2009**, *54*, 4889.
- (26) Kobayashi, K.; Usami, N.; Porcel, E.; Lacombe, S.; Le Sech, C. *Mutat. Res., Rev. Mutat. Res.* **2010**, *704*, 123.
- (27) McMahan, S. J. *J. Phys. Chem. C* **2011**, *115*, 20160.
- (28) Zafriou, O. C. *Mar. Chem.* **1990**, *30*, 31.
- (29) Roa, W.; Zhang, X. J.; Guo, L. H.; Shaw, A.; Hu, X. Y.; Xiong, Y. P.; Gulavita, S.; Patel, S.; Sun, X. J.; Chen, J.; Moore, R.; Xing, J. Z. *Nanotechnology* **2009**, *20*, 37.
- (30) Kong, T.; Zeng, J.; Wang, X. P.; Yang, X. Y.; Yang, J.; McQuarrie, S.; McEwan, A.; Roa, W.; Chen, J.; Xing, J. Z. *Small* **2008**, *4*, 1537.